A COMPARISON OF FRAGMENTATION CALCULATIONS WITHIN MICROSCOPIC AND MACROSCOPIC FRAMEWORKS*

D.J. Morrissey †

Nuclear Science Division
Lawrence Berkeley Laboratory
Berkeley, California 94720

ABSTRACT

The calculation of the isotopic production cross sections from high energy heavy ion reactions has proceeded along two divergent paths. From the regime of relativistic heavy ion reactions comes the abrasion-ablation model which is dependent on the quick nature of these collisions and the separation of the reactant nuclei into participants and spectators. From the intermediate energy regime comes the intranuclear cascade model where the reaction is treated as a sum of nucleon-nucleon scattering events inside a nuclear potential well. Both frameworks are able to treat projectile as well as target fragmentation. In this presentation the results of both model calculations will be compared to recent experimental data for the fragmentation of 213 MeV/A ^{40}Ar projectiles by ^{12}C nuclei and for the fragmentation of ^{209}Bi target nuclei by a 400 MeV/A ^{20}Ne beam. These comparisons show the importance of the statistical decay process in determining the distribution of final products as well as the deficiencies of the two models.

The recently reported production of neutron-rich light isotopes in relativistic heavy ion reactions[1] has brought new interest into the calculation of the fragment production cross sections. These calculations arose in the regimes of high energy proton induced reactions and cosmic ray physics and were carried over into the new field of relativistic heavy ion reactions.[2] Just as their backgrounds are different, the calculational approaches to fragmentation reactions are also very different. In this paper we will present the results of a microscopic intranuclear cascade-evaporation calculation and a macroscopic abrasion-ablation calculation for projectile fragments from the reaction of 8.52 GeV ^{40}Ar with ^{12}C and for target fragments from the reaction of 8.0 GeV ^{20}Ne with ^{209}Bi. The comparison of the results of these model calculations with each other and with experimental data will be especially useful because the forms of both models that we have used are parameter free.[3] The comparisons are also interesting because they should shed light on those factors that play important roles in the production of these fragments.

The collision of the relativistic heavy ion (RHI) projectile with the target nucleus is treated as a two-step process in the Monte Carlo cascade calculation. A fast step occurs with cascading collisions of nucleons from one reaction partner inside the nucleus of the other partner, which is followed by a slow statistical evaporation of the primary fragments after

the fast cascading nucleons have escaped or have been captured by the primary fragments. The calculation is made using an extension[4] of the intranucleon cascade code,[5] VEGAS, for proton induced reactions which has been modified to treat two colliding nuclei. The two nuclei have diffuse nuclear density distributions and Fermi motion of the nucleons is also included. The neutron or proton nature of the collision partners is selected at random in proportion to their number in the nucleus. The impact parameter is also selected at random, and the final cross sections were integrated over impact parameter. The primary fragments are subsequently individually deexcited using a version of the Dostrovsky, Fraenkel and Friedlander statistical model Monte Carlo calculations.[6,4] The excitation energy of each fragment was obtained from the fast cascade code.

In the abrasion-ablation view of the collision of the RHI with a target nucleus the two nuclei are taken to be uniform hard spheres which move on straight line trajectories.[7] Those nucleons that lie in the region of overlap of the two nuclei are sheared off in the abrasion (or fast) stage of the collision. The spectator fragments of the target (and projectile) which consist of the nucleons that were outside the region of overlap are assigned an excitation energy that is proportional to their excess surface area. This is the minimum excitation energy that such fragments would be expected to have, and increases due to frictional forces are likely to be present. The variance

of the neutron to proton ratio can be calculated in the statistical limit[7] or through ground state fluctuations of normal nuclear matter.[8,9]

The results of these calculations can be seen in Fig. 1 for the case of fragmentation of a 213 MeV/A ^{40}Ar with ^{12}C. Both the cross sections from the fast stage of the reaction (primary) and the cross sections from the statistical stage (final) are shown for three different calculations. In Fig. 1A and 1C the abrasion-ablation model was used along with an uncorrelated[7] and a highly correlated[8] neutron-proton distribution, respectively. These products are allowed to deexcite and produce the distributions of products seen in Figs. 1B and 1D. The distribution of nuclei produced by the fast cascade are shown in Fig. 1E and after deexcitation in Fig. 1F. Comparison of the primary fragment cross section distributions from the three models show that these distributions are very dissimilar. The difference in the correlations among the removed nucleons can be seen in the width of the Z distributions at constant mass number. The two uncorrelated distributions are approximately twice as wide as the correlated one. However, the final residue cross sections are quite similar. This comes about because of the relatively large amounts of excitation energy deposited in the primary fragments by the collision process. For comparison the measured data of reference 1 is shown in Fig. 2. In general, the data is well reproduced by

the correlated abrasion-ablation and the cascade-evaporation models, the uncorrelated abrasion-ablation final distribution is too broad. For these light nuclei the final isotopic distributions bear the characteristics of the valley of beta stability and pre-equilibrium features of the distributions are washed out by the statistical process.

The influence of the statistical process may be lessened by considering the fragmentation of a high mass nucleus because the valley of beta-stability is broader and statistical evaporation of charged particles is inhibited. In Fig. 3 we present the results for the final product cross sections for gold and thallium isotopes from the reaction of 400 MeV/A ^{20}Ne with ^{209}Bi. Only the correlated abrasion-ablation results (solid curve) and the uncorrelated cascade-evaporation results (histograms) are shown. Large differences are immediately apparent between the two calculations. The uncorrelated final product distribution is approximately three times as wide as the correlated one, and although flatter contains slightly more cross section. For comparison the results of reference 10 for the production of these isotopes are shown by the solid points. The cross sections were measured radiochemically and corrected for beta-decay feeding; unfortunately, the most neutron deficient nuclei had half-lives too short for measurement.[10] The abrasion-ablation calculation predicts nuclei which are too neutron excessive, this may be due to an underestimation of the excitation energy of the fragments. The

width of the distribution is not obtainable from the measurements and must wait for future experiments.

In conclusion we can say that the measured isotope production cross sections for the framentation of ^{40}Ar on a ^{12}C target are in general agreement with the absolute predictions of the uncorrelated cascade-evaporation model and the correlated abrasion-ablation model. Because of the high excitation energies deposited in the primary fragments by the fast interactions, and the nature of statistical processes, the pre-equilibrium features of the distributions are supressed in the fragmentation of light nuclei. These features are visible with fragmentation of heavy nuclei, but measured results for such processes are incomplete.

References

*This work was supported by the Nuclear Physics Division of the U.S. Department of Energy under contract No. W-7405-ENG-48.

†The calculations presented here are taken in part from reference 3, and we would like to acknowledge the contributions of the other authors of reference 3 for their assistance in these calculations. We would also like to thank Dr. K. Aleklett for the use of his data prior to publication.

1. T.J.M. Symons et al., Phys. Rev. Lett. 42, 40 (1979), and V.P. Viyogi et al., Phys. Rev. Lett. 42, 33 (1979).
2. For review see A.S. Goldhaber and H.H. Heckman, Ann. Rev. Nucl. Part. Sci. 28, 161 (1978).
3. D.J. Morrissey, L.F. Oliveira, J.O. Rasmussen, G.T. Seaborg, Y. Yariv and Z. Fraenkel, Phys. Rev. Lett., submitted for publication, and Lawrence Berkeley Laboratory report LBL-8964.
4. Y. Yariv and Z. Fraenkel, to be published.
5. K. Chen, Z. Fraenkel, G. Friedlander, J.R. Grover, J.M. Miller and Y. Shimamoto, Phys. Rev. 166, 949 (1968).
6. I. Dostrovsky, Z. Fraenkel and G. Friedlander, Phys. Rev. 116, 683 (1959).
7. See for example, L.F. Oliveira, R. Donangelo and J.O. Rasmussen, Phys. Rev. C19, 826 (1979), and references therein.

8. D.J. Morrisey, W.R. Marsh, R.J. Otto, W. Loveland and G.T. Seaborg, Phys. Rev. C18, 1267 (1978).

9. J.P. Bondorf, G. Fai and O.B. Nielson, Phys. Rev. Lett. 41, 391 (1978), Nucl. Phys. A312, 149 (1978).

10. K. Aleklett, private communication.

Figure Captions

1. The primary fragment isotopic production cross sections for ^{40}Ar fragmentation are shown in (A), (C) and (E) for the three models discussed in the text. The final products, after statistical deexcitation, are shown in (B), (D) and (F).
2. The data from reference 1 is shown as a contour diagram for comparison to the calculations represented in Fig. 1.
3. The calculated values of the production cross sections for gold and thallium isotopes are shown for the cascade-evaporation (histograms) and for the abrasion-ablation (solid curve) calculations. The data from reference 10 is shown as the solid points.

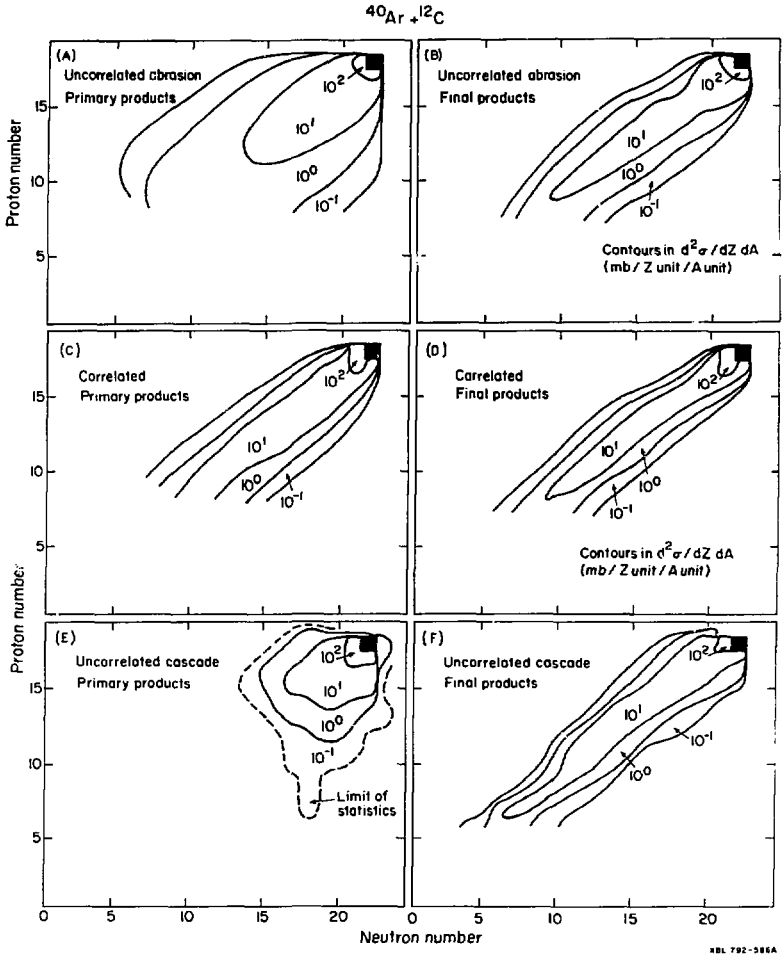
$^{40}Ar + ^{12}C$
(A)
Uncorrelated abrasion
Primary products
(B)
Uncorrelated abrasion
Final products
Contours in $d^2\sigma/dZ\,dA$
(mb/Z unit/A unit)
(C)
Correlated
Primary products
(D)
Correlated
Final products
Contours in $d^2\sigma/dZ\,dA$
(mb/Z unit/A unit)
(E)
Uncorrelated cascade
Primary products
Limit of statistics
(F)
Uncorrelated cascade
Final products
10^2
10^1
10^0
10^{-1}
Proton number
Neutron number
0
5
10
15
20
XBL 792-586A

Fig. 1

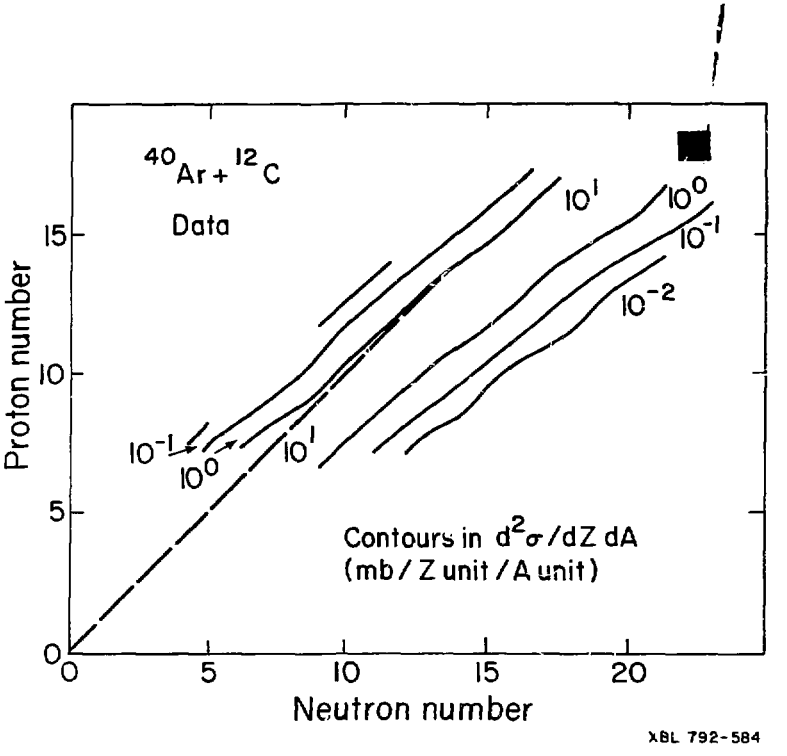
$^{40}Ar + ^{12}C$
Data
10^{1}
10^{0}
10^{-1}
10^{-2}
10^{-1}
10^{0}
10^{1}
Contours in $d^2\sigma/dZ\,dA$
(mb / Z unit / A unit)
Proton number
Neutron number
0
5
10
15
20
XBL 792-584

Fig. 2

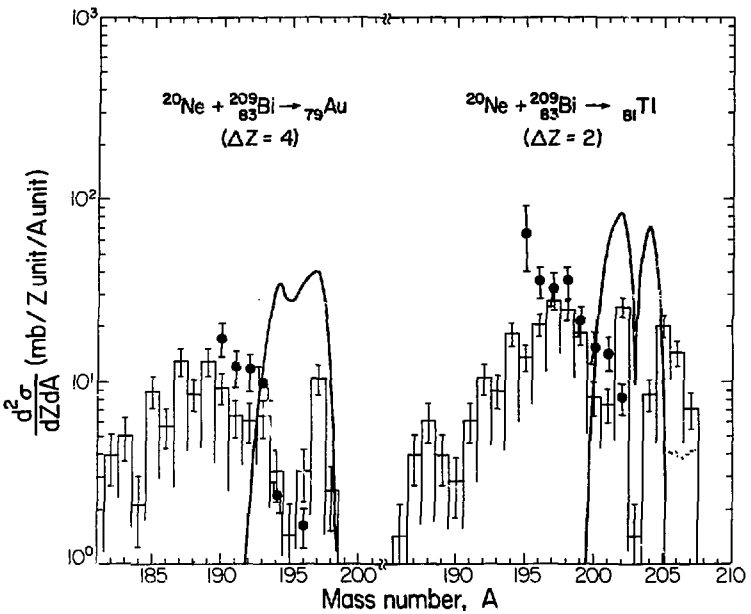

XBL 797-2125

Fig. 3